The Dan David Center for Human Evolution and Biohistory Research

ACTIVITY REPORT 2018 – 2019

Submitted by
Prof. Israel Hershkovitz
Dr. Hila May
Dr. Rachel Sarig
Sackler Faculty of Medicine

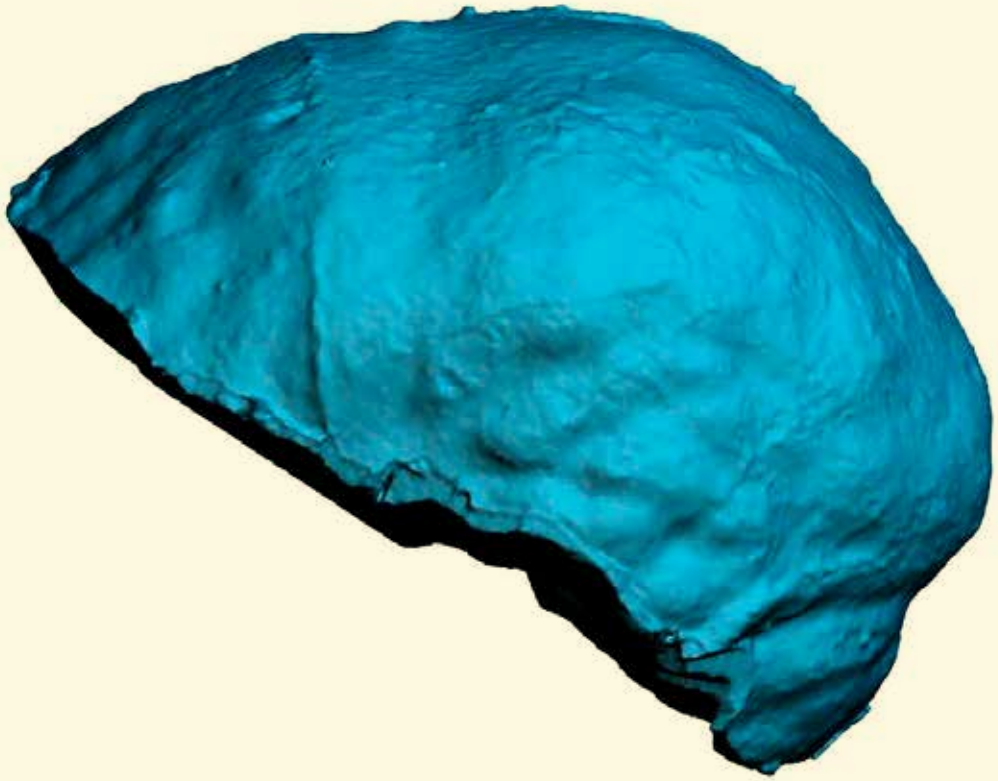

TEL AVIV UNIVERSITY
אוניברסיטת תל אביב

●●● TABLE OF CONTENTS

Major Activities

Excavation Reports

MAJOR ACTIVITIES

RUNNING RESEARCH PROJECTS

1. Nesher-Ramla Skull (140,000 Years Old). Research Project: Early Presence of the Neanderthals in the Levant.
2. Geulla Cave Teeth (100, 000 Years Old). Research Projects: Neanderthal-Homo Sapiens Introgression.
3. Har Safsuf Cave Human Remains: Research Project: Human Migration in the Chalcolithic.
4. Natufian and Neolithic Mandibles. Research Project: Micro-Evolutionary Trends in the Masticatory System during the Holocene.
5. Manot Cave Hominins: Research Project: Who were the Levantine Aurignacians?
6. Natufian, Neolithic and Chalcolithic Femora. Research Project: Changes in Physical Burden during the Holocene.
7. Ancient DNA Studies. Research Project A: Anatolian Migration during the Chalcolithic, Research Project B: The Geographical Origin of the Natufian People, Research Project C: The Jews from the Second Temple Period and their Association to Present Jewish Populations.
8. The Teeth from Qesem Cave: Research Project: Who were the Achelu-Yabrudians?
9. The Qafzeh Cave Hominins. Research Project: Mal Occlusal or Mal Adaptation?
10. Tel Rehov Human Remains. Research Project: The Assyrian in Israel.

MULTI-YEARS FIELD PROJECTS

1. Manot Cave Excavation (Early Upper Paleolithic)
2. Tinshemet Cave Project (Middle Paleolithic)
3. Skhul Cave Project (Middle Paleolithic)
4. Tabun Cave Project (Middle Paleolithic)

NEW EXCAVATIONS

1. **Timna:** Who were the workers in the copper mines at Timna?
2. **Yotvata:** Who was buried in the mausoleum at the top of the hill?
3. **Yarmout:** Prepottery Neolithic site, early farmers in the Judean hills
4. **El-wad:** Natufian hunter-gatherers in Mount Carmel
5. **Safsuf:** Chalcolithic burials deep in caves site in the Upper Galilee

RESEARCH GRANTS RECEIVED

International Foundations	**Amount**
Irene Levi-Sala CARE Archaeological Foundation	5,000$
National Geographic Society	34,000$
Leakey Foundation	24,000$
Wenner-Gren Foundation	20,000$
Broad-ISF	378,000$
Bi-national Science Foundation	220,000$
Australian Research Council	254,000$
Gerda-Henkel Foundation	68,000€
Israeli Foundations	**Amount**
Schreiber Foundation Sackler Faculty of Medicine TAU	40,000 NIS
Israel Science Foundation (ISF)	651,000 NIS
Israel Science Foundation (ISF)	576,156 NIS
Recanati Medical Research Foundation, Sackler Faculty of Medicine	70,000 NIS
Private Donation	**Amount**
Ronnie Chan	48,000$

PUBLICATIONS 2018-2019

Feldman M, Fernández-Domínguez E, Reynolds L, Baird D, Pearson J, Hershkovitz I, May H, Goring-Morris N, Benz M, Gresky J, Bianco RA, Fairbairn A, Mustafaoğlu G, Stockhammer PW, Posth C, Haak W, Jeong C, Krause J. (2019). Late Pleistocene human genome suggests a local origin for the first farmers of central Anatolia. *Nature Communication*. Mar 19, 10 (1):1218. doi: 10.1038/s41467-019-09209-7.

Abbas J, Hamoud K, Peled N, Hershkovitz I. (2018). Lumbar Schmorl's Nodes and Their Correlation with Spine Configuration and Degeneration. Biomed Res Int. 2018 Nov 7; 2018:1574020. doi: 10.1155/2018/1574020. eCollection 2018.

Hershkovitz I, Duval M, Grün R, Mercier N, Valladas H, Ayalon A, Bar-Matthews M, Weber GW, Quam R, Zaidner Y, Weinstein-Evron M. (2018). Response to Comment on "The earliest modern humans outside Africa". *Science*. 2018, Oct 26, 362(6413). doi: 10.1126/science.aat8964. PMID: 30361343.

Ezra, D., Slon, V., Kedar, E., Masharawi, Y., Salame, K., Alperovitch-Najenson, D., Hershkovitz, I. (2018). The Torg ratio of C3-C7 in African-Americans and European-Americans: A skeletal study. *Clin Anat*. Sep 9. doi: 10.1002/ca.23269. [Epub ahead of print], PMID: 30198179.

Ezra, D., Hershkovitz, I., Salame, K., Alperovitch-Najenson, D., Slon, V. (2018). Osteophytes in the cervical vertebral bodies (C3-C7) – Demographical perspectives. *Anat Rec.* Oct 5. doi: 10.1002/ar.23901. [Epub ahead of print], PMID: 30290057.

Harney, E., May, H., Shalem, D., Rohland, N., Mallick, S., Lazaridis, I., Sarig, R., Stewardson, K., Nordenfelt, S., Patterson, N., Hershkovitz, I.* & Reich, D*. (2018). Ancient DNA from Chalcolithic Israel reveals the role of population mixture in cultural transformation. *Nature communications* DOI: 10.1038/s41467-018-05649-9 (* equal contribution).

Zohar, I., Dayan, T., Goren, M., Nadel, D., Hershkovitz, I. (2018). Opportunism or aquatic specialization? Evidence of freshwater fish exploitation at Ohalo II – A waterlogged Upper Paleolithic site. *PLOS one* 13(6) e0198747.

Hershkovitz, I., Weber, G. W., Quam, R., Duval, M., Grün, R., Kinsley, L., Ayalon, A., Bar-Matthews, M., Valladas, H., & Weinstein-Evron, M. (2018). The earliest modern humans outside Africa. *Science*, 359(6374), 456-459.

Sella Tunis, T., Sarig, R., Cohen, H., Medlej, B., Peled, N., May H. (2017). Sex estimation using computed tomography of the mandible International Journal of Legal Medicine. I*nternational Journal of Legal Medicine*, 1-10,

Sella-Tunis, T., Pokhojaev, A., Sarig, R., O'Higgins, P., May, H. (2018). Human mandibular shape is associated with masticatory muscle force. *Scientific Reports*, 8(1), 6042.

May, H., Sella-Tunis, T., Pokhojaev, A., Peled, N., Sarig, R. Changes in mandible characteristics during the terminal Pleistocene to Holocene Levant and their association with dietary habits. *Journal of Archaeological Science: Reports*, 2018.

Pokhojaev, A., Habashi, W., May, H., Schulz-Kornas, E., Shvalb, N., Sarig, R., Examination of the Interproximal Wear Mechanism: Facet Morphology and Surface Texture Analysis. *Journal of Dental Research* 97: 1445-1451 doi: 10.1177/0022034518785140.

MSc AND PhD STUDENTS AT THE DAN DAVID CENTER FOR HUMAN EVOLUTION AND BIOHISTORY RESEARCH

PhD Students	Research
Einat Kedar,	Sackler School of Medicine, Anatomy and Anthropology.
Sarah Borgel, PhD PI D. Hila May	Studies bone histology, biomechanics, prehistory of the Levant and human evolution.
Hadas Avni-Levine, PhD PI D. Hila May	Studying the shape of the proximal femur and how changes in its shape, can teach us about population differences, human evolution and pathologies.
Mila Rajapova (Hejja), PhD	Studying Anatomy and Anthropology.
Ruth Kallevag, PhD PI D. Hila May	Studying the shape of the lumbar curvature during growth, and its association with intervertebral disc and vertebral parameters.
Victoria Roul, PhD PI D. Hila May	Studying the variation in femoral curvature and the shape of the distal femur in modern and prehistoric populations, and its association with different pathologies and types of physical activity.
Amal Bader Farraj, PhD PI Dr. Rachel Sarig	Current project is to define molars' roots morphology evolutionary changes and their relation to function.
Itay Nudel, PhD PI Dr. Rachel Sarig	Focusing on the formation of Secondary Dentinan as a possible hallmark for applied masticatory forces.

PhD Students	Research
Waseem Habashi, PhD PI Rachel Sarig	Research explains the relation between surface Fluoride concentration and bio-mechanical forces in the mouth. We use a Fluoride Electrode that determines F concentration, Nanofocus Microscope in order to calculate the amount of material loss from surface of teeth, and motion stimulator for grinding/clinching movements mimicking.
Michal Peer, PhD	Studying Anatomy and Anthropology.
MSc Students	**Research**
Samuel Francis, MS PI D. Hila May c	Studying the shape of the femur and its relationship to the muscles around it, investigating whether femoral shape is a good indicator of physical activity and lifestyle.
Yoli Bitterman, MSc PI Dr. Rachel Sarig	Studying restorative dentistry's basic skills Department of Oral Rehabilitation.
MD Student	**Research**
Efrat Gilat, (Research project)	Sackler Faculty of Medicine

FOREIGN RESEARCHERS VISITING THE DAN DAVID CENTER FOR HUMAN EVOLUTION AND BIOHISTORY RESEARCH (SINCE 2018)

- Rolf Quam – Binghamton University (SUNY), Binghamton, NY, USA
- Rebeka Remitilova – Czech Republic
- Antonio Profiko – Italy
- Yerusleb Brozak – Czech Republic
- Anne-Marie Tillier – University of Bordeau, France
- Marrie-Anton – France
- Danni Continioun – France

ACTIVE COLLABORATION PROJECTS WITH FOREIGN RESEARCHERS

- Gerhard Weber – University of Vienna, Austria
- Anne-Marie Tillier – Université Bordeaux, France
- Dominique Grimaud-Hervé – Muséum national d'Histoire naturelle, Paris, France
- David Reich – Harvard University, US
- Svante Pääbo – Max Planck Institute for Evolutionary Anthropology, Leipzig, Germany
- Johannes Krause – Max Planck Institute for the Science of Human History, Jena, Germany
- Rolf Quam, Binghamton University, US

- Bruce Latimer, Case Western Reserve University, Ohio, US
- Luca Fiorenza – Monash University, Australia
- Paul O'Higgins – The University of York, UK

ACTIVE COLLABORATION PROJECTS (INCLUDING JOINT RESEARCH GRANTS) WITH ISRAELI ARCHAEOLOGISTS FROM DIFFERENT UNIVERSITIES

- Dr. Yossi Zaidner – Hebrew University
- Dr. Uri Davidovich – Hebrew University
- Dr. Dina Shalem – Kinneret College
- Prof. Ofer Marder – Ben Gurion University
- Prof. Mina Weinstein Evron – Haifa University
- Dr. Reuven Yeshurun – Haifa University
- Dr. Dani Nadel – Haifa University
- Dr. Ron Shimelmitz – Haifa University
- Dr. Omri Barzilay – Israel Antiquities Authority
- Prof. Udi Weiss – Bar Ilan University
- Dr. Guy Stibel – Tel Aviv University
- Prof. Erez Ben-Yosef – Tel Aviv University
- Prof. Avi Gopher – Tel Aviv University

COLLABORATION AGREEMENTS WITH DIFFERENT INSTITUTIONS

1. Department of Anthropology, University Of Vienna
2. Israel Antiquity Authority

The Dan David Center established a formal relationship with the Department of Anthropology at the University of Vienna, they are our partners in the study of human fossils from Israel.

EXCAVATION REPORTS
TABUN CAVE

New Excavation at Tabun Cave
Report for 2018-19

In collaboration with Mina Weinstein-Evron[1] and Ron Shimelmitz[1]

[1] Zinman Institute of Archaeology, University of Haifa, Mount Carmel 3498838, Haifa, Israel

Israel Antiquities Authority permit: G15-2018

Israel Nature and Parks Authority permit: 18-ℵ021

INTRODUCTION

Tabun Cave is located at the western edge of Mount Carmel, at the opening of Nahal Me'arot. It was first excavated between 1929 and 1934 by D.A.E. Garrod (Garrod and Bate, 1937). The total depth of sediments in the cave is 25 meters, in which Garrod divided the stratigraphical sequence into seven layers, ranging from the Lower Paleolithic to the late Middle Paleolithic. Three of these layers are attributed to the Middle Paleolithic, including Layer D of the early Middle Paleolithic, Layer C of the middle Middle Paleolithic and Layer B of the late Middle Paleolithic. Each of these layers represents a different phase in the Levantine Middle Paleolithic (Shea, 2003; Hovers, 2009).

During the 1930's excavation several human remains were retrieved from layers B and C. The most famous of these is C1 – the Neanderthal women that was found in the interface between layers C and B (McCown and Keith, 1939). While its attribution to a specific layer was left in question by Garrod (Garrod and Bate, 1937), it is most often assigned today to Layer B (Bar-Yosef and Callander, 1999). Additional human remains were found within Layer B (McCown and Keith, 1939), including dental remains (Coppa et al., 2005). The finding of Neanderthal remains in Layer B correlates with other sites dated to the late Middle Paleolithic (Bar-Yosef et al., 1992; Hovers et al., 1995; Akazawa et al., 1999; Been et al., 2017). Nevertheless, the presence of *Homo sapiens* in Manot, during roughly the same timeframe, is also of note (Hershkovitz et al., 2015).

Since the 1930's, two other excavation expeditions at Tabun Cave were conducted. One by Arthur Jelinek between 1967 and 1971 (Jelinek et al., 1973; Jelinek, 1982), and the second by Avraham Ronen between 1975 and 2003 (Ronen et al., 2011). Ronen excavated the Lower Paleolithic layers of the cave, while Jelinek excavated a 10-meter step section at the middle of the former section made by Garrod. Jelinek's section covered Garrod's Layers E-C, ranging from the Lower Paleolithic to the middle of the Middle Paleolithic. Layer B was not included in Jelinek's trench and as such, this part of the cave was not excavated since 1934 despite its enormous significance. The potential of a new excavation is further echoed in that studies of aNDA from the last decade hypothesize the Levantine late Middle Paleolithic as the time and place of gene-flow between Neanderthals and *Homo sapiens* (Sankararaman et al., 2012; Kuhlwilm et al., 2016).

In 2017, Mina Weinstein-Evron and Ron Shimelmitz, the University of Haifa and Israel Hershkovitz, from Tel Aviv University initiated a new excavation project in Tabun Layer B. The excavation project is being supported by the Dan David and Gerda Henkel Foundations. Through the excavation, we aim to:

1. Better understand the stratigraphy of this part of the sequence including its environment of deposition and post-depositional processes.
2. Provide for the first time a comprehensive chronological frame for this part of the stratigraphy using a variety of methods.
3. Reconstruct the paleoenvironment and human exploitation patterns using a set of studies of biotic remains.
4. Track anthropogenic signatures within the sediments such as the extent of fire use using micromorphology.
5. Identify patterns in material culture referring to cognition, landscape exploitation, site use and the transformation of socially learned knowledge.
6. Attempt to provide a better context for the human remains found at the site in the 1930's in order to better understand the nature of interaction between Neanderthals and *Homo sapiens* during the late Middle Paleolithic.

THE EXCAVATION TEAM INCLUDES

Archaeobotany: Mina Weinstein Evron, Zinman Institute of Archaeology, University of Haifa.

Lithic Technology: Ron Shimelmitz, Zinman Institute of Archaeology, University of Haifa.

Physical Anthropology: Israel Hershkovitz, Hila May, Rachel Sarig, Sackler Faculty of Medicine, Tel Aviv University.

OSL Dating: Norbert Mercier, Institut de Recherche sur les Archéomatériaux, Université Bordeaux Montaigne.

TL dating: Helene Valladas, Laboratore des Sciences du Climat & de l'Environment, Université Paris-Saclay, Gif Sur Yvette.

ESR dating: Mathieu Duval and Rainer Grün, Research School of Earth Sciences, The Australian National University, Canberra, Australia.

Fauna: Reuven Yeshurun and Meir Orbach, Zinman Institute of Archaeology, University of Haifa.

Microfauna: Lior Weissbrod and Tal Fried, Zinman Institute of Archaeology, University of Haifa.

Chiroptera: Prof. Ivan Horáček, Department of Zoology, Charles University in Prague.

Isotopic analysis: Julia Lee-Thorpe, Research Laboratory for Archaeology & the History of Art, School of Archaeology, University of Oxford.

Micromorphology: David Friesem, Zinman Institute of Archaeology, University of Haifa, and Ruth Shahack-Gross, Department of Maritime Civilization, University of Haifa.

Use-wear: Iris Groman-Yaroslavski, Use-Wear Analysis Laboratory, Zinman Institute of Archaeology, University of Haifa.

Tephra analysis: Dustin White, Department of Geography, Royal Holloway, University of London.

Phytoliths: Dan Cabanes, Department of Archaeology, Rutgers the State University of New Jersey.

Charcoals: Valentina Caracuta, Università del Salento.

(Additional experts will join the project as it proceeds)

LOCATION OF THE NEW EXCAVATION

The new excavations at Tabun Cave focuses on Layer B and its transition to the underling Layer C. The eastern part of the inner room (Fig. 1), which has not been excavated since 1934, constitutes the locality of the new excavation. In order to protect the stepped section, we enter the cave from the chimney through a special ladder that runs along ca. 13 meters from the plateau above the cave to the top of the sediments remained (Fig. 2). The ladder is attached to the wall of the cave and does not have any contact with the archaeological sediments. In order to maintain the safety of the excavation team we fenced the border of the excavation and each excavator attended a working in height course. A safety line was also constructed from the inner chamber to the opening of the cave below.

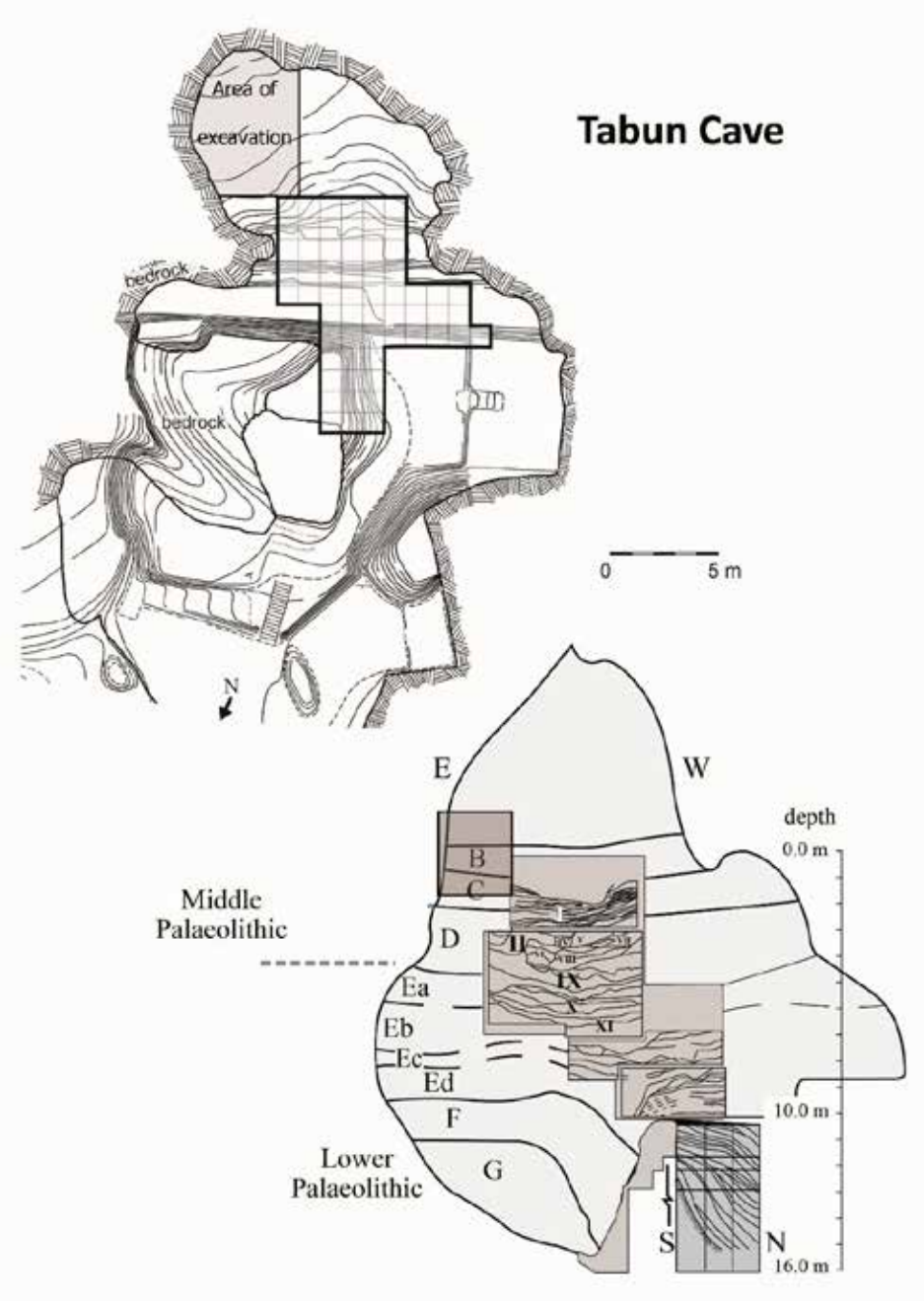

Fig. 1: Tabun Cave and the area of the new excavation
(the main locality of former excavations by Jelinek and Ronen is marked as well).

Fig. 2: The entrance to the inner chamber that runs through a 13 meters ladder originating from the chimney's top at the plateau of Mount Carmel.

Garrod left at the end of her excavation at Tabun a set of steps running from the inner chamber to the external chamber (Fig. 3). In the inner room, this includes three close-by steps with small differences in elevation between them. Steps 1 and 2 of this stepped section did not preserve well, and the sediments are inclining from the south to the north, creating a small talus with only minor portions of the most upper parts of Steps 1 and 2 remained intact. We placed a safety net, which fences our excavation area, near the edge of Step 3. The visible remaining portions of the upper parts of steps 1-2 include cemented sediments along the southern and eastern walls of the cave. The erosion of the steps left by Garrod occurred through the exposure to the elements following the end of excavation in 1934. A roof over the chimney was placed only in the late 1960's by A. Jelinek, which stopped the erosion of the steps in the inner chamber.

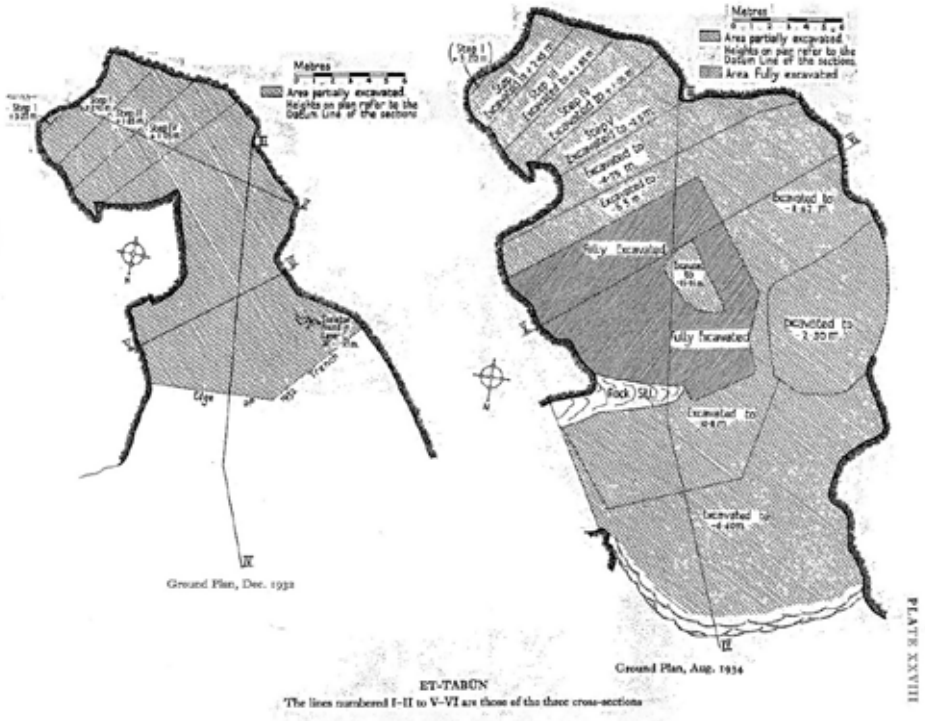

Fig. 3: The stepped section left by Garrod at the inner chamber at the end of the excavations in 1934 (After Garrod and Bate 1937: Pl.XXVIII).

A new grid and a labeling system of squares was defined for our new project, in which the current area of exaction is at the intersection of Columns K and L and Rows 1-5. The grid is structured on the coordinates of the former excavations. We changed its parameters however since using the former system of square labeling and metrics did not enable defining new squares as former squares were labeled in running numbers from 1 to almost 100. Furthermore, new squares would have resulted in negative numbers in terms of the grid metrics (Shimelmitz et al., 2014: Fig. 1). The new system enables us to define squares in areas left blank by the former excavations. The selected locality of excavation covers the area from the southern wall of the cave to the intermediate chamber. The surface at this locality inclines from south to north with the south at a height of ca. 3m above datum and north at 1.9m above datum. In 2018, excavation was conducted in squares K4, K5, L2(a,b), L3, L4 and L5. The grid is not perfectly aligned towards the north, rather to the opening of the cave. In the photographs, the north arrow is aligned toward the northern part of the net and not towards the true north.

EXCAVATION METHODS AND RECOVERY OF FINDS

Excavation was conducted by dividing each square meter into four sub-squares (50x50cm). All sediments were wet sieved through 1mm mesh and artifacts larger than 2cm were recorded with a total station providing three coordinates. Sediment samples were retrieved from each level of excavation and their locality was also recorded by the total station. Stones of various sizes that were recovered in high numbers in our excavation, were drawn and their bottom and top elevations provided by the total station. Photogrammetry was used to record the surface of excavation at different stages of our season. In order to best preserve use wear and residue if present, Lithic artifacts were not washed. In order to enable dosimetry, teeth identified in the field suitable for ESR dating, were accompanied by a sediment sample from the locality where they were retrieved. The sediments from a full sub-square from each spit were meticulously examined for charcoal remains.

THE 2018 EXCAVATION

The second season of excavation at Tabun Layer B was performed during February 2018. An additional fieldwork at Tabun was also conducted later for micromorphology (15.3.2018), OSL dosimeter removal (31.5.18) and Tephra sampling (26.6.2018). Excavation was conducted in six squares (1m^2) defined as K4, K5, L2, L3, L4 and L5 that their excavation initiated in 2017 (excavation in square L2 was made only at the two northern sub-squares). The 2018 excavations at squares K-L/4-5 started at an elevation of 1.55m above datum, reached in 2017 and ended up in elevation 1.25-1.45. Excavation in squares L3 and L2 was performed at elevation 2.32-2.00 m above datum (Fig. 4).

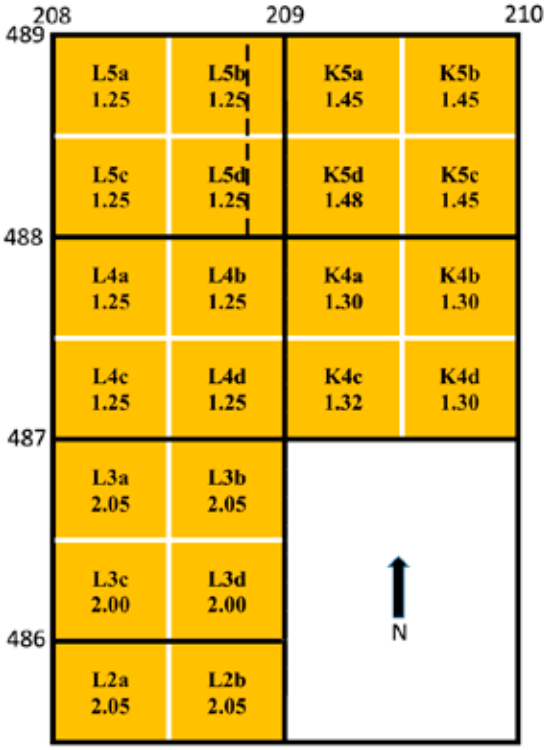

Fig. 4: The grid of excavation with elevation above datum at the end of the 2018 excavation. The numbers outside the frame indicate northing and easting. Note that the eastern portion of L5b-d remained as well at elevation 1.45 m (north points to the excavation north, following the early excavations grid).

Within the excavated volume we identify four layers, during 2018 excavation focused on Layers III-IV (Fig. 5):

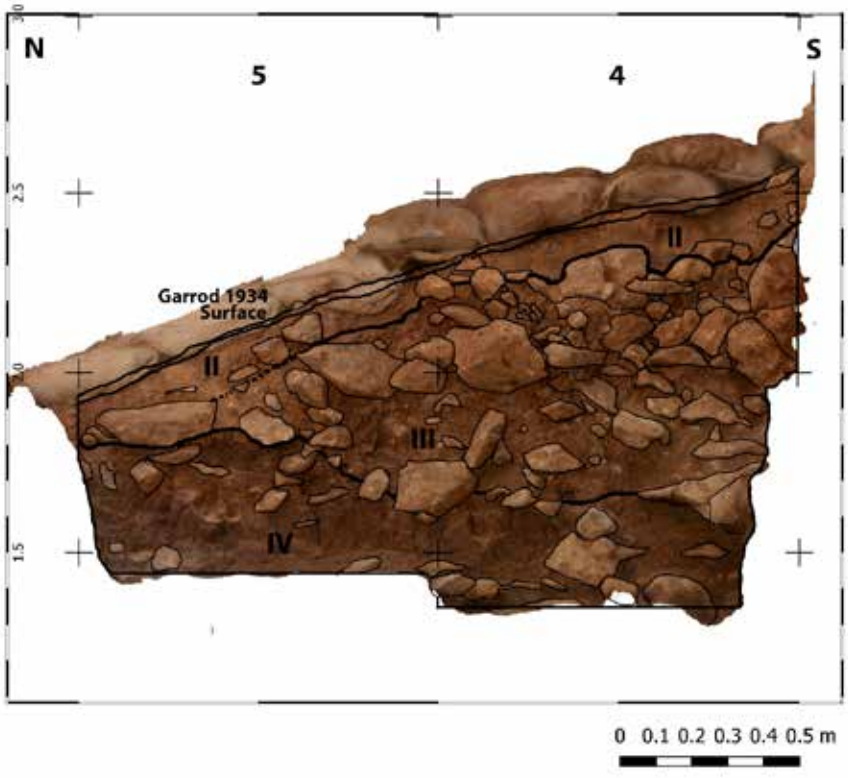

Fig. 5: South-north section, showing layers II-IV and the stony nature of Layer III in particular.

Layer I

This layer is partly cemented and spreads along squares K1, K2, K3, L1 and L2 of our excavation area (Fig. 6). It includes many stones in various sizes as well as a high density of faunal material. Only a few lithics were observed in this layer. The layer, which is close to the cave walls, was not excavated in 2017-2018. Its volume, according to the section made in L2(a,b) just below the cemented sediments (Fig. 7), is ca. 20-30cm and it inclines towards the north. Among the faunal material a mandibles of fallow deer and some bones in articulation were noted. During 2018, we partly cleaned its eroding upper part according to the grid and registered all identified faunal material by three coordinates.

Fig. 6: The area of excavation at the end of the 2018 season (facing east). Note the party cemented layers at the south east part of the inner room.

Fig. 7: The southern section of L2. Note at the very upper part the cemented layer I. Also note the stony nature of the sediments.

Layer II

This layer is composed of soft sediments. The sediments are gray to light brown in color and include a high density of bones and several lithics as well. The layer is ca. 10-15 cm thick, with an especially high representation in squares K4, L4 and L3. This layer as well inclines towards the north. Microfauna is prevalent in this layer. The sediments include a high presence of terra-rossa and they crumble into small chunks of 1-2 cm in size. Stones of various sizes, ranging from few mm to 30cm are frequent within this layer. This layer was not excavated during 2018, as no new squares were opened. However, in a few places, section straightening work, following stone removals, the geomorphological work and the tephra examination at the end of the 2017 season, was conducted.

Layer III

This is a dark brown clay layer that includes many stones of various sizes within it (Figs. 8-9). Its depth is still unclear. The artifacts in it include primarily bones, especially at the upper part, however stone tools and waste in small numbers were found as well. A clear decline in the amount of bones and lithics is witness in compare to layers I-II. The numerous limestones in this layer are assumed to be the result of the partial collapse of the cave roof, which created the current massive chimney that is located above the excavation area. While the process of the creation of the chimney started at the base of Jelinek's Unit I (Layer C; Jelinek et al., 1973), the massive concentrations of stones suggest that a significant expansion of the chimney occurred during the time of Layer B. The sediments are darker and more compact. During the excavation, the sediments fragmented into large chunks. The density of stones increases, in comparison to layer II and stones are spread all over the area of excavation of Layer III. Thus, Layer III can be described as a "stony layer", probably reflecting an episode of a significant extension and collapse of the chimney, and less as a hominin living occupation. At the lower part of Layer III, excavated in squares K-L/4-5, finds are not prevalent but flint artifacts are more common than bones (both appear in small numbers). Bones however appear in a higher number at squares L2-3. In Square L3c at elevation 2.03, a mandible and several fallow deer teeth were found. It is still unclear whether the more abundance of bones in these squares is due to the proximity to the wall of the cave, or whether it results from still constituting the upper part of Layer III. It was also apparent to us that the stone texture changes with depth. While many of the upper stones bear some brown-orange crust, the stones from the lower part lack it. More rounded stones were also found in the lower part in contrast to the upper part where many of the stone are angular. The sediment found between the stones in L5 and especially at its northern part (sub squares a-b) are free and easily removed by a brush only.

Fig. 8: Area of excavation at elevation 1.50 above datum (facing south). Note the stony layer III in the surrounding sections. Also, note that its concentration and depth is greater at the western side, in which its base is still not attained (Squares L4-5).

Fig. 9: The area of excavation at elevation 1.50 m above datum (facing west).

Layer IV

The sediments of layer IV are characterized as hard dark brown clay and include a lower amount of stones. The layer is very compact and hard to excavate. It includes few finds as in the lower part of Layer III. Among the artifacts found, lithics are more common. Within the sediments, charcoal was observed at several localities, with the clearest presence in square K5a. The highest concentration of charcoals, which also include the presence of dark and gray sediments, was found at the border between squares K5 and L5 (Figs. 10-11). In order to really inspect the presence of a possible combustion feature in this locality, we left intact square K5 and a strip of 20 cm from the eastern part of square L5 at elevation 1.45 cm above datum for the micromorphological study that was conducted at the end of the season. It is of note, that while it may indicate the presence of a combustion feature, no clear intact hearth was found. Squares in which charcoals were identified during the excavation were hand sorted for charcoal material (before the wet sieving), supervised by Dr. Valentina Caracuta. The stones of Layer IV lack crust. Some stones were found to be half eroded, with their external surface being yellowish in color and crumbling while the internal mass is more solid (Fig. 12-13) (samples were kept).

At elevation, 1.35 m above datum stones became frequent again in square K4. The stone in this locality are heavily eroded. In square K4, a cluster of a charcoal, a flint core and a flat lithic artifact was found. The possibility that the new stony concentration represents a new layer (V) will be evaluated according to its extension in the following season (Figs. 14-15).

Fig. 10: A patch of black sediments including several charcoals at the southern intersection between squares K5 and L5 and the upper part of Layer IV.

Fig. 11: several patches of black sediments in which few charcoals were also found.

Fig. 12: Yellow clusters were found in Layer IV, especially near the eastern part of squares K5 and K4. The yellow clusters are soft and crumbling, and currently assumed to constitute eroded stones. Samples were taken (picture facing east).

Fig. 13. A surface from Layer IV demonstrating the presence of both stones and the yellow patches that are assumed to constitute eroded stones.

Fig. 14: Area of excavation at elevation 1.35 above datum. In order to examine the area with black sediments we stopped the excavation in square K5 and 20 cm of the eastern part of square L5 at elevation 145.

Fig. 15: Square K4 at elevation 1.35 above datum. At the lower part of layer IV we encountered large stones again. It is still unclear whether they should indicate the beginning of Layer V.

PHOTOGRAMMETRY

During the excavation we took several sets of multiple pictures for creating 3D models using photogrammetry. These sets were taken on the 18th, the 22nd and the 25th of February (e.g. Fig. 5, 16 that were extracted from the 3D models).

Fig. 16: Snapshot of the photogrammetry 3D model from the end of the excavation, showing the eastern profile.

PRELIMINARY NOTES REGARDING THE FINDS

The finds within the excavated layers include primarily animal bones. The most conspicuous species is the fallow deer (*Dama mesopotamica*), although gazelles are also well represented. A protruding presence of young individuals is of note. Stone tools and waste (Fig. 17) were found to some extent in all four layers, but are relatively few in compare to the amount of bones. The lithic finds include tools such as scrapers, as well as waste of production and cores. Microfauna is also well preserved within the sediments. Shells of land snails were also found. A list of the units subjected to charcoal examination is provided in Table 1. Charcoal was found in nine units, and their analysis is underway by V. Caracuta.

Fig. 17: Lithics from Layers III-IV, including Levallois flake (1), tools (2-5) and a Levallois point (6).

Table 1: List of units handpicked for charcoals during the 2018 season

K4d	1782	133	handpicked	IV	no charcoal
K5a	1958	151	handpicked		no charcoal
K4d	1794	130	handpicked	IV	no charcoal
K4b	541	144-140	handpicked	IV	no charcoal
K5b	1448	144	handpicked	IV	no charcoal
K5a	493	149-145	handpicked	IV	
K5a	1455	144	handpicked	IV	
K4b	1717	133	handpicked	IV	
K4d	1673	136	handpicked	IV	no charcoal
L4b	1790	133	handpicked		no charcoal
L4b	1751	136	handpicked	IV	no charcoal
L4b	566	135-130	handpicked	IV	no charcoal
K4d	1799	130	handpicked	IV	no charcoal
K4b	1716	134	handpicked	IV	
K5b	490	147-145	handpicked	IV	no charcoal
L4b	1800	126	handpicked	IV	
L4b	1778	135	handpicked	IV	no charcoal
L4b	1796	130	handpicked	IV	no charcoal
L4b	568	130-125	handpicked	IV	no charcoal
L4a	1752	135	handpicked	IV	no charcoal
K4a	1777	130	handpicked	IV	no charcoal
K5a	1454	145	handpicked	IV	
L4b	1464	148	handpicked	IV	
K4d	546	141-135	handpicked	IV	
K4d	1672	135	handpicked	IV	no charcoal
K4d	569	135-130	handpicked	IV	

DATING PROGRAM

The new dating program involves four radiometric methods including Optically Stimulated Luminescence (OSL) of sediments and U-Series using laser ablation (N. Mercier, University of Bordeaux Montaigne), Thermoluminescence technique (TL) of burnt flint pieces (H. Valladas, Gif-sur-Yvette) and Electron Spin Resonance (ESR) of teeth (M. Duval and Rainer Grün, Research Centre of Human Evolution, Griffith University).

The samples for dating were taken from the Tabun Cave covering the entire range of the Middle Paleolithic of the cave, mostly obtained from Jelinek's section. The location of the three dating samples from Layer B and dosimeters is provided in Tables 2-3. The three OSL dosimeters placed at 2017 were removed on 30.5.2018. The samples are currently under analysis at the University of Bordeaux Montaigne.

Table 2: OSL samples from Tabun Cave

OSL No.	Layer	section	E	N	Z
Tabun OSL 19	New layer I		208.15	485.5	3.07
Tabun OSL 20	New Layer III		208.6178	485.5945	2.6204
Tabun OSL 21	New Layer II		209.3871	486.8697	2.5419

Table 3: Dosimeter placed in Tabun Cave at October 2017 and removed at May 2018

Dosimeter no.	Layer	Square and face	Lab number	E	N	Z
Tabun dos. 19	New layer I	L2south	99	208.44	485.56	2.9197
Tabun dos. 20	New Layer III	L2south	c321	208.8	485.5	2.6
Tabun dos. 21	New Layer II	K3north	c384	209.69	486.92	2.512

GEOLOGICAL RESEARCH

Four bulk sediment samples (TBS 18-107 to 110) and two undisturbed block sediment samples (TAB 18-18 and 19) were collected from the new excavation area of Tabun B, square K5.

The bulk sediment samples were analyzed using FTIR spectroscopy for identification of the major mineral components and in particular for identifying exposure to high temperatures (>450°C). The results are listed in the table 4.

Table 4: FTIR spectroscopy of samples retrieved during the 2018 season

Sample	Description	Major Minerals	Notes
TBS 18-107a	Brown sediment	Cl(na)>>Q>org	Decalcified?
TBS 18-107b	Black sediment	Cl(a)>>>Ca, Q, org	Burnt to >500°C
TBS 18-108a	Brown yellow sediment	Cl(na)>Ca, CHAP>Q, org	Phosphatised
TBS 18-108b	Dark brown sediment	Cl(na)>>Ca, Q>org	Terra rossa
TBS 18-109	Brown yellow sediment	Cl(na)>>>Ca, Q, org	Terra rossa
TBS 18-110a	Black sediment	Cl(na)>>>Ca, Q, org	Only charred <500°C
TBS 18-110b	Brown sediment	Cl(na)>>Ca, CHAP>Q, org	Phosphatised
TBS 18-110c	Black sediment	Cl(a?)>>>org, Q> Ca	Not clear if burnt to >500°C

[Cl=clay; (na)=nonaltered; (a)=altered; Q=quartz; Ca=calcite; CHAP=carbonated hydroxylapetite; org=organic matter]

Overall, the results of the FTIR suggest that the concentration of black sediment could be related to deposition of fire residues. More information will be available through micromorphological analysis of the two block sediments sampled from this locus once thin sections will be ready.

In addition, three complementary undisturbed block sediment samples (TAB 18-20 to 23) were collected from the upper eastern profile from Jelinek's excavation in order to record the upper part of layer Tabun C and the transition to Tabun B.

CRYPTO TEPHRA ANALYSIS

Another method of understanding the chronological horizons along the long sequence of the Middle Paleolithic of Tabun Cave is by searching crypto tephra that are microscopic ash traces of volcanic eruptions. The method is based on volcanic ash from each eruption, is characterized by a specific chemical fingerprint that can be traced. As such, we can correlate the same exact chronological horizons (distal localities) among different sites and provide a clear date which origin is performed at the place of eruption (proximal locality). In order to explore this field of research Dustin White (Royal Holloway University of London) had taken a large set of samples retrieved from eight columns during 2017. Following the initial results that identified tephra at the upper part of our new area of excavation, Dustin White sampled during 2018 additional three columns at the upper part of our excavation and identified within them tephra remains as well (Tables 5-7). Columns 9-10 were sampled at the southern face of square L2 (Fig. 18). Column 11 was sampled at the eastern part of square K4.

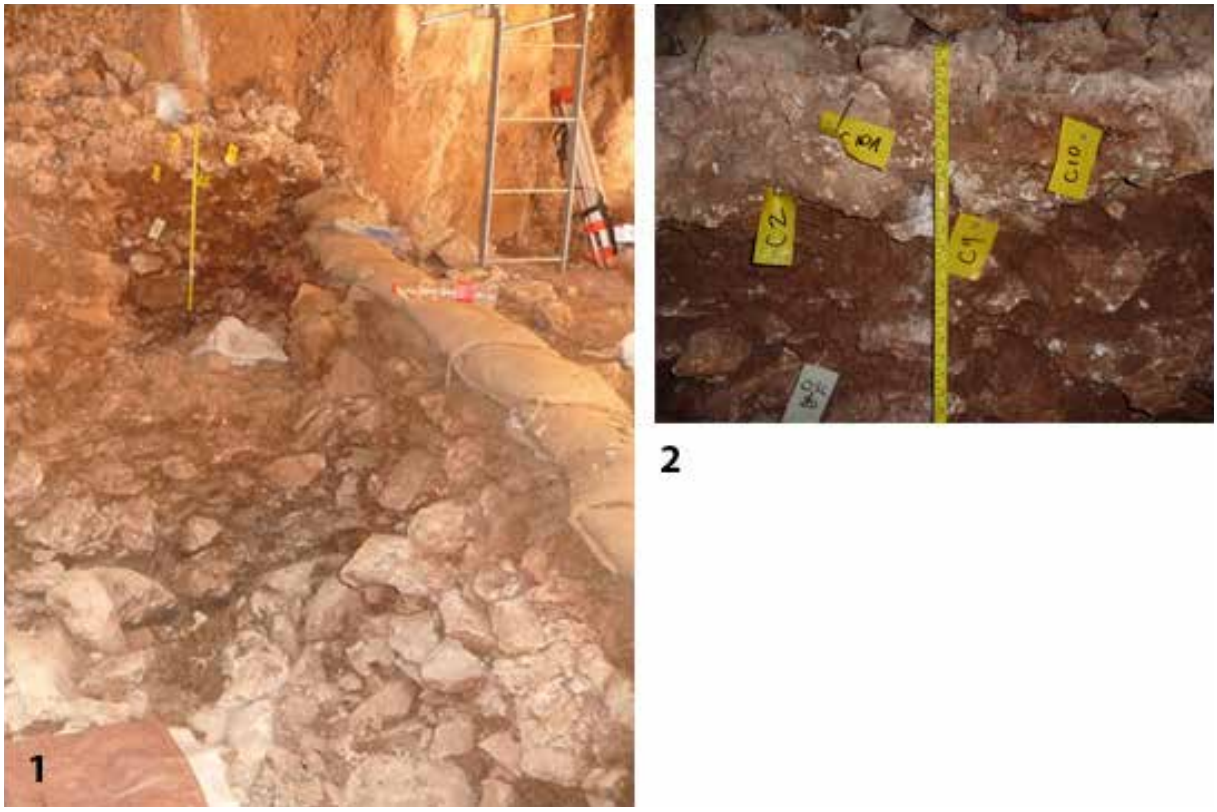

Fig. 18: Tephra column 9 extracted from the southern wall of square L2, sampling layers 1 and 3.

Table 5: Tephra Column 9

Column 9 - Square L2, Quadrant C/D boundary, South Section (Z tape measure = 3.07m depth below datum), samples collected 25/				
Sample No.	**db Z (cm)**	**Corrected db datum (m)**	**Stratigraphic Unit**	**Comments**
1	56-54	**2.51-2.53**	III	Base of Column 1
2	54-52	**2.53-2.55**	III	
3	52-50	**2.55-2.57**	III	
4	50-48	**2.57-2.59**	III	
5	48-46	**2.59-2.61**	III	
6	46-44	**2.61-2.63**	III	
7	44-42	**2.63-2.65**	III	
8	42-40	**2.65-2.67**	III	
9	40-38	**2.67-2.69**	III	
10	38-36	**2.69-2.71**	III	
11	36-34	**2.71-2.73**	III	
12	34-32	**2.73-2.75**	III	
13	32-30	**2.75-2.77**	III	
14	30-28	**2.77-2.79**	III	
15	28-26	**2.79-2.81**	III	
16	26-24	**2.81-2.83**	III	
17	24-22	**2.83-2.85**	III	
18	22-20	**2.85-2.87**	III	Breccia contact/stone?
19	20-18	**2.87-2.89**	III	Mainly stone
20	18-16	**2.89-2.91**	III	Stone + remnant of crumbly Unit II?/Top o

Table 6: Tephra Column 10

Column 10 - Square L2, Quadrant C, South Section (Z tape measure = 3.07m depth below datum), samples collected 25/06/2018				
Sample No.	**db Z (cm)**	**Corrected db datum (m)**	**Stratigraphic Unit**	**Comments**
1	30-28	**2.77-2.79**	III	Base of Column 10
2	28-26	**2.79-2.81**	III	
3	26-24	**2.81-2.83**	III	
4	24-22	**2.83-2.85**	III	
5	22-20	**2.85-2.87**	III	
6	20-18	**2.87-2.89**	III	
7	18-16	**2.89-2.91**	III	
8	16-14	**2.91-2.93**	III/II contact?	Thin lenses of Unit II present in this part o
9	14-12	**2.93-2.95**	Contact with breccia (Unit I)	Top of Column 10

Table 7: Tephra Column 11

Column 11 - Square K4, Quadrant B, East Section (Z tape measure = 2.04m depth below datum), samples collected 25/06/2018				
Sample No.	**db Z (cm)**	**Corrected db datum (m)**	**Stratigraphic Unit**	**Comments**
1	70-65	**1.34-1.39**	IV	Base of Column 1
2	65-60	**1.39-1.44**	IV	
3	60-55	**1.44-1.49**	IV	
4	55-50	**1.49-1.54**	IV	
5	50-45	**1.54-1.59**	IV	
6	45-40	**1.59-1.64**	IV/III contact	
7	40-35	**1.64-1.69**	III	
8	35-30	**1.69-1.74**	III	
9	30-25	**1.74-1.79**	III	
10	25-20	**1.79-1.84**	III	
11	20-15	**1.84-1.89**	III	
12	15-10	**1.89-1.94**	III - stone	Top of Column 11

REFERENCES

Akazawa, T., Muhesen, S., Ishida, H., Kondo, O., Griggo, C., 1999. New discovery of a neanderthal child burial from the Dederiyeh Cave in Syria. Paléorient. 25, 129–142.

Bar-Yosef, O., Callander, J., 1999. The woman from Tabun: Garrod's doubts in historical perspective. Journal of human evolution. 37, 879–885.

Bar-Yosef, O., Vandermeersch, B., Arensburg, B., Belfer-Cohen, A., Goldberg, P., Laville, H., Meignen, L., Rak, Y., Speth, J.D., Tchernov, E., Weiner, S., 1992. The excavations in Kebara Cave, Mt. Carmel. Current Anthropology. 33, 497–550.

Been, E., Hovers, E., Ravid, E., Malinski-buller, A., Agha, N., Mayer, D.E.B., Benazzi, S., Hublin, J., 2017. The first Neanderthal remains from an open-air Middle Palaeolithic site in the Levant. Scientific Reports. 7.

Coppa, A., Grün, R., Stringer, C., Eggins, S., Vargiu, R., 2005. Newly recognized Pleistocene human teeth from Tabun Cave, Israel. Journal of Human Evolution. 49, 301–315.

Garrod, D.A.E., Bate, D.M.A., 1937. The Stone Age of Mount Carmel, I, Clarendon. ed. Oxford.

Goldberg, P., 1973. Sedimentology, Stratigraphy and Paleoclimatology of et-Tabun Cave, Mt. Carmel, Israel. University of Michigan.

Hershkovitz, I., Marder, O., Ayalon, A., Bar-matthews, M., Yasur, G., Boaretto, E., Caracuta, V., Alex, B., Frumkin, A., Goder-goldberger, M., Gunz, P., Holloway, R.L., Latimer, B., Lavi, R., Matthews, A., Slon, V., Mayer, D.B., Berna, F., Bar-oz, G., 2015. Levantine cranium from Manot Cave (Israel) foreshadows the first European modern humans. Nature. 520, 216–219.

Hovers, E., 2009. The Lithic Assemblage of Qafzeh Cave. Oxford University Press, Oxford.

Hovers, E., Rak, Y., Lavi, R., Kimbel, W.H., 1995. Hominid remains from Amud Cave in the context of the Levantine Middle Paleolithic. Paléorient. 21, 47–61.

Jelinek, A.J., 1982. The Tabun Cave and Paleolithic man in the Levant. Science (New York, N.Y.). 216, 1369–1375.

Jelinek, A.J., Farrand, W.R., Haas, G., Horowitz, A., Goldberg, P., 1973. New excavations at the Tabun cave, Mount Carmel, Israel, 1967-1972 : A preliminary report. Paléorient. 1, 151–183.

Kuhlwilm, M., Gronau, I., Hubisz, M.J., de Filippo, C., Prado-Martinez, J., Kircher, M., Fu, Q., Burbano, H.A., Lalueza-Fox, C., de la Rasilla, M., Rosas, A., Rudan, P., Brajkovic, D., Kucan, Ž., Gušic, I., Marques-Bonet, T., Andrés, A.M., Viola, B., Pääbo, S., Meyer, M., Siepel, A., Castellano, S., 2016. Ancient gene flow from early modern humans into Eastern Neanderthals. Nature. 530, 429–433.

McCown, T.D., Keith, A., 1939. The Stone Age of Mount Carmel II. Clarendon Press, Oxford.

Ronen, A., Gisis, I., Tchernikov, I., 2011. The Mugharan Tradition reconsidered. In: Le Tensorer, J.M., Jagher, R., Otte, M. (Eds.), The Lower and Middle Paleolithic in the Middle East and Neighboring Regions. ERAUL, Liège, pp. 121–130.

Sankararaman, S., Patterson, N., Li, H., Pääbo, S., Reich, D., 2012. The date of interbreeding between Neandertals and modern humans. PLoS Genetics. 8.

Shea, J.J., 2003. The Middle Paleolithic of the East Mediterranean Levant. Journal of World Prehistory. 17, 313–394.

Shimelmitz, R., Kuhn, S.L., Ronen, A., Weinstein-Evron, M., 2014. Predetermined flake production at the Lower/Middle Paleolithic boundary: Yabrudian scraper-blank technology. PloS one. 9, e106293.

EXCAVATION REPORTS
TINSHEMET CAVE

New Excavation at Tinshemet Cave
Report for 2018-19

In collaboration with Yossi Zaidner

Institute of Archeology, the Hebrew University

The Research Team:

Archaeology: Yossi Zaidner[1], Oz Varoner[2], Marion Prevost[1], Laura Centi[1], Asaph Levy[1], Chen Zeigen[1], Mika Ulman[1].

Paleoanthropology: Israel Hershkovitz[3], Hila May[3], Rachel Sarig[3]

Zooarchaeology: Reuven Yershurun[4], Kathryn Pocklington[4]

OSL dating: Naomi Porat[5]

Micro-morhology: Ruth Shahack-Gross[6]

Cryptotephra: Dustin White[7]

[1]Institute of Archaeology, the Hebrew University of Jerusalem, [2] Department of Bible, Archaeology and the Ancient Near East, Ben-Gurion University of the Negev, [3]Department of Anatomy and Anthropology, Dan David Center for Human Evolution and Biohistory Research, Shmunis Family Anthropology Institute, Sackler Faculty of Medicine, Tel Aviv University [4] Zinman Institute of Archaeology, University of Haifa [5]Geological Survey of Israel [6] Department of Maritime Civilizations, University of Haifa, Haifa, [7] Faculty of Arts and Humanities, University of Southampton.

INTRODUCTION

Tinshemet Cave, also known as Mugharet al-Watwat (Stekelis, 1942), is located in central Israel, near the modern city of Shoham. The cave is located on a moderate slope on the east bank of the Nahal Bet-Arif stream, approximately 20 meters above the riverbed (Figure 1).

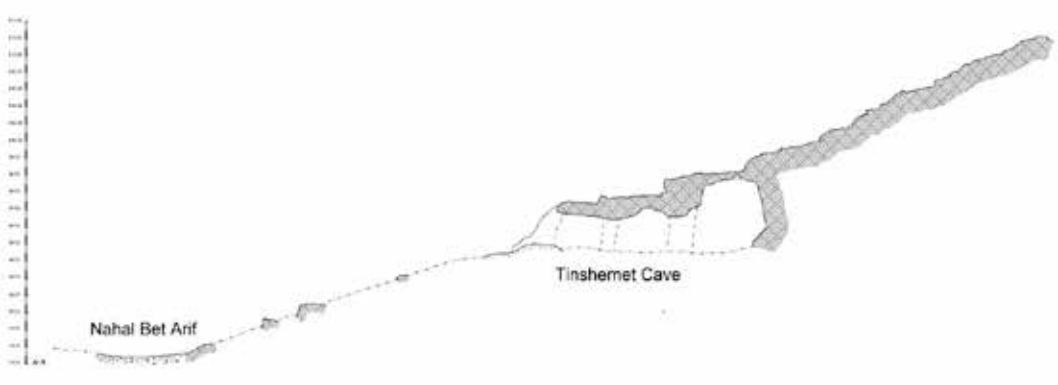

Figure 1. The section of the slope where Tinshemet Cave is located.

The 2018 season at the Tinshemet Cave had three main goals:

1. Better understanding of the site stratigraphy and the human culture and behavior by enlarging the archaeological and paleoanthropological assemblages. This goal was achieved by the continuation of excavations in the areas excavated in the previous seasons, (first chamber and terrace), and by opening new squares on the terrace near the southern wall of the cave (henceforth, "the rock shelter"; fig 2);
2. The second goal, was to complete the excavation in the squares adjacent to the remains of the Tinshemet 2 skeleton. The block that contains the Tinshemet 2 skeleton, is ready for extraction and transportation to further work at the Dan David Laboratory, Tel Aviv University;
3. The third objective concerns with the dating of the site and site formation processes. As for the dating of the site, in addition to the OSL samples taken in the 2016 season, and to the TL samples taken in the 2017 season, a new set of OSL samples were taken from different areas of the cave. Site formation processes were studied within the perspective of micromorphology and cryptotephra.

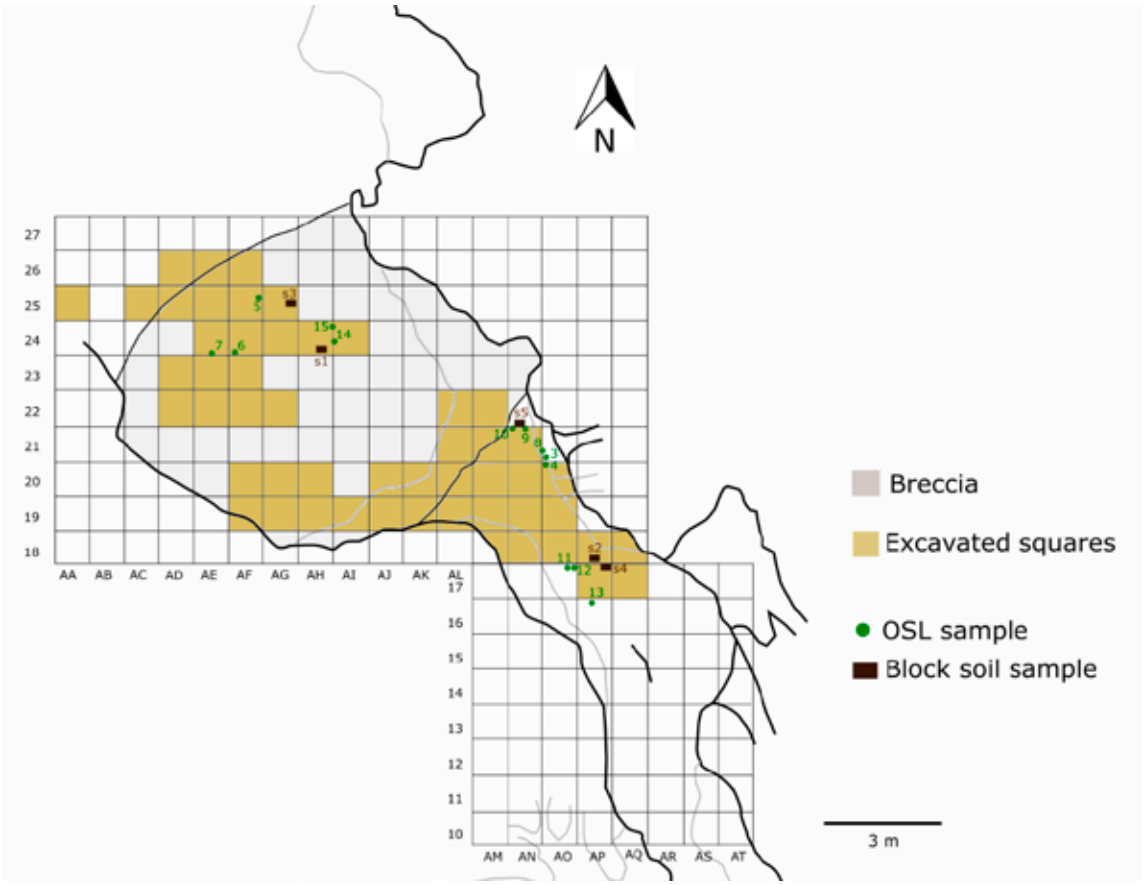

Figure 2. General plan of the areas excavated during 2018 season.

First Chamber

The excavation in the first chamber was conducted in three "sub-areas" (fig. 3). The northern part of the chamber (sq. AM, AN 20-21) is characterized by a soft in-situ sediment contains Middle Paleolithic artifacts. Since the Tinshemet 1 skeleton (see 2017 report) was exposed in these squares, our aims here were a better understanding of the stratigraphy of Tinshemet 1 and to search for additional human remains in this area.

Figure 3. The first chamber and the squares excavated in 2018 season.

In sub-square AN 21a, around 15 cm below the Tinshemet 1, human skull fragments were discovered (figs 3, 4). Few fragmented faunal remains, flint artifacts, small pieces of charcoal were associated with the skull. The human skull fragment was identified as "Tinshemet 4" and was removed at the end of the season. The sediments surrounding "Tinshemet 1" and Tinshemet 4" are similar light brown fine grain sediments.

Figure 4. Skulls remains in squares AM 21b (Tinshemet 5 and 6) and AN 21a (Tinshemet 4).

In sub-square AM21b 15 cm above the elevation of the Tinshemet 4 skull, two additional human remains (skull fragments) were discovered; named "Tinshemet 5" and "Tinshemet 6" (fig. 3). For now, part of "Tinshemet 5" is still unexposed, another fragment identified as a frontal part of the skull was removed (fig. 5).

Figure 5. Skull fragment of "Tinshemet 5".

Tinshemet 6 skull is located near the section of the cave that was not excavated. We enlarged the excavations area and opened square AM 22 to enable the excavation of the skull. Since we did not finish the exposure of Tinshemet 6, the fragments of the skull were not retrieved. Flint artifacts and fragmented animal bones were also found in the association of the remains.

An interesting concentration of flint artifacts is located between "Tinshemet 5 and 6" (Fig. 6). This concentration is composed of four large flint flakes vertically positioned. They were found in the section with the northern square AM 22, therefore they were not removed during the 2018's season. The flint artifacts

differ significantly in their size from other flint artifacts found in those squares. The artifacts appear near the human remains and are concentrated in a small area suggesting that they were deliberately placed there in a kind of a "cache" connected to the skull remains.

Figure 6. The concentration of flint artifacts near "Tinshemet 5 and 6".

The middle part of the chamber or the "passage" leading to the second chamber is represented by the squares AO 18-19-20 (fig. 2). In the 2017 season, we started to expose the bedrock to the east. The aim of the 2018 season in this area was to check the depth and extensiveness of the Middle Paleolithic sediments in this area. At the end of the season, we exposed an accumulation of large stones in the squares mentioned above (fig. 7). The sediments between the stones show small quantities of artifacts.

Figure 7. Concentration of large stones in the 'passage' in the first chamber.

During the 2017 season of excavations, we exposed black sediment suspected to be a hearth, in the southern part of the first chamber (squares AP, AO 18). Therefore, during the 2018 season, we opened the adjacent squares to the south (squares AP, AO 17). The upper 10 cm layer containing small rounded stones was removed. This stony layer was composed of mixed pottery fragments, modern glass, flint artifacts and modern micro-fauna (mostly bates). Additional 25-30 cm of compact dark brown sediments were excavated. These black sediments contained a few lithic artifacts and animal bones. A low density of artifacts and no evidence for anthropogenic activities suggests that this layer is composed of cave, non-anthropogenic sediments. The black color could represent manganese and which reflects water activity. The micromorphological studies also suggest that this layer is not anthropogenic.

Finally, the square AM 18, where an isolated human tooth was retrieved during the 2017 season of excavations, was fully excavated and the "bedrock" was exposed. The upper part of the section (upper 10-15 cm), are disturbed by roots. The sediments are soft and not compact. The square was found to be rich in flint artifacts and fragmented animal bones. We also noted the presence of several manuports (rounded limestone "pebble") in this square (Fig. 8).

Figure 8. Angular stones associated with rounded pebbles (possible manuports).

The "Rock Shelter"

The "rock shelter" is a new area opened in the 2018 season. This area is comprised of some 18m^2 stretching to the S-W of the entrance to the first chamber (squares AF-AL/19-21 on the excavation grid) where the inward curving of the cave wall creates the semblance of a small rock shelter. Prior to excavation, a naturally exposed stretch of hard breccia sloped down from the N-E corner, topsoil and vegetation obscured its extent in the S and W squares of the area. Therefore, the goal of this season was to investigate the extent of the hard breccia in this area. A North-South section on the eastern boundary of the area with the first chamber showed a suggested possible preservation of soft Middle Paleolithic sediments near the cave wall. After the removal of the topsoil in several squares, a brecciated layer began to revel (fig 9). The newly exposed breccia is comprised of two elements: an upper crust of loose breccia, softened by the weathering and borrowing of roots; and a hard breccia, just like the one exposed at the terrace. A test excavation of the breccia in square AI-AJ/19 revealed that the loose breccia is removed relatively easily and is of a maximal thickness of 10cm. In the western part of the area, there is an abrupt elevation drop of the hard breccia. A testing of square AH19 revealed a depression in the breccia, filled with dark brown top soil, with fist sized angular stones. An excavation of ca. 45cm failed to reach the bottom of this depression due to narrowing of its walls.

Figure 9. The rock shelter at the end of the 2018 season.

The topsoil in this area is rich in heavily patinated lithic material. Faunal remains are also present in the topsoil, with a mixture of recent and fossilized bones. Throughout the topsoil, pottery sherds and metal objects where unearthed. Both hard and soft breccia contained embedded lithics and fossilized faunal remains. Special finds include a large fragment of a bovid long bone with a percussion mark, laid horizontally on top of the soft breccia (fig.10) and a large piece of red ochre.

Figure 10. Long bone with percussion mark.

To summarize, most of the Middle Paleolithic sediments in the rock shelter area appear to have undergone similar diagenetic processes to those of the terrace, leaving a mass of thoroughly brecciated archaeological sediments. The breccia seems to have undergone some braking and erosion, predominantly in the western half of the area, where a depression is yet to be further exposed. In the southern extremity of this area, close to the cave wall, it is yet to be determined whether some soft sediments were preserved under large collapsed stones. Further works should focus on excavation of the hard breccia in order to establish a stratigraphy of this area and investigate relations to the adjacent terrace and first chamber.

The Terrace

The excavation in the terrace continued this year and generally followed the same stratigraphy as described in previous seasons – a mixed top soil layer covering several distinguishable brecciated layers. The excavation on the terrace was dedicated to three main goals. The first goal was to excavate around the Tinshemet 2 skeleton in order to allow its safe removal. The second was to define the borders of the B1 surface – the uppermost breccia layer. The third was to understand the stratigraphic relations between the different breccia layers and to begin mapping their horizontal expansion

The excavation around Tinshemet 2 skeleton took place in three squares – AF24, AG25 and AH24.

In AF24, we excavated layers B2 (a brecciated layer with many rocks and few anthropogenic finds) and the underlying B3 (a brecciated layer with few finds and few stones).

In AG25, we excavated the bottom part of layer B1 in the entire square (a brecciated layer under topsoil with many flint items, burnt bones and ochre chunks). After the removal of layer B1, we continued further down to layers B2, and B3 (as described above).

Square AH24 was opened this year. The square is located on the slope between the modern-day cave entrance and the Tinshemet 2 skeleton. The excavation in this square was conducted in a much harder breccia. Two layers were discerned; a top hard breccia layer with sparse finds, and a lower hard breccia with many finds, including flint items, bones, ochre and a rare basalt groundstone tool (fig. 7). It remains open whether this layer is the continuation of the previously defined B1 surface. During the 2018 season, we finished the excavation of the western and northern sections around Tinshemet 2 skeleton (fig. 12) and prepared it for an extraction.

Figure 11. Basalt groundstone from the AH24 square on the terrace.

Figure 12. "Tinshemet 2" and the squares excavated at the 2018 season.

As mentioned in the 2017 report, the B1 surface is a high-density concentration of finds, including flint items, bones and ochre. During the 2018 season of excavations, this surface was excavated in squares AE23/AF23. Additionally, the top soil was removed in squares AE22/AF22 (south of the visible B1 layer) in order to define the limits of this surface. Below this top soil layer is a breccia (lower in elevation than the B1 surface) which was not excavated. In this breccia, there was a round depression, similar to those already visible in the brecciated slope between the modern-day cave entrance and the terrace – probably attesting to an ancient water drip activity inside the cave or at its dripline.

In order to extend our general understanding of the breccia layer in the context of the whole site, we opened two new squares AA25 and AG22.

Square AA25 is located at the western part of the terrace. Two layers were discerned during the excavation. The first is the topsoil that consists of compact brown sediments with a mixture of pottery and flint items. The second layer contains of light brown sediments with many stones, some flint items and bones (and lacks pottery). This layer shows no similar features to the squares in the eastern part of the terrace and most probably represents mixed sediments that were eroded down the slope. Below this layer limestone bedrock was reached. All layers are tilted from SE to NW (fig.13).

Figure 13. Square AA25.

Square AG22 is located on the slope between the modern-day cave entrance and the terrace. Shortly after beginning excavation, a surface with high density of flint items was reached (fig 14), and excavation ceased.

Figure 14. The surface exposed in square AG22.

Dating

In addition to the OSL samples taken in the 2016 season, a new set of samples was collected during the 2018 season (fig 2). The samples were collected in the vicinity of the human remains in the first chamber and on the terrace, from the southern part of the first chamber, and from layer B1 on the terrace.

In addition, sediment blocks for micromorphology and samples for cryptotephera were collected in the first chamber and on the terrace. Cryptotephra are microscopic grains of volcanic ash that can be chemically attributed to known volcanic eruptions and thus provide high resolution absolute dating along the anthropogenic sequence.

Lithics

The lithic assemblage of the Tinshemt Cave counts for a few thousand pieces. Although detailed analysis of the flint assemblage has not yet been conducted, several field observations were made. The most common type of flint used at Tinshemet Cave is the Mishash Formation flint. This flint is found in both primary and secondary sources near the site. The dominating technology for flint knapping is the Levallois method as expressed by the cores and the detached pieces. The most common scar pattern on the flake is centripetal scar pattern. The retouched pieces occur in low frequency. The majority of the tools are irregularly retouched, with very few side-scrapers.

Fauna

The taxonomic composition (Table 1) is varied and includes several large body species such as aurochs (*Bos primigenius*), mountain gazelle (*Gazella gazella*), equids (*Equus* sp.; large-bodied), Mesopotamian fallow deer (*Dama mesopotamica*), wild goat (*Capra* sp.), red deer (*Cervus elaphus*) and wild boar (*Sus scrofa*). The two most frequent species are gazelle and aurochs, followed by equids, cervids and the caprine although the last two species mentioned above are in small quantity. Notably, small mammals are rare and yet, tortoise and snake remains were found during the 2017 season.

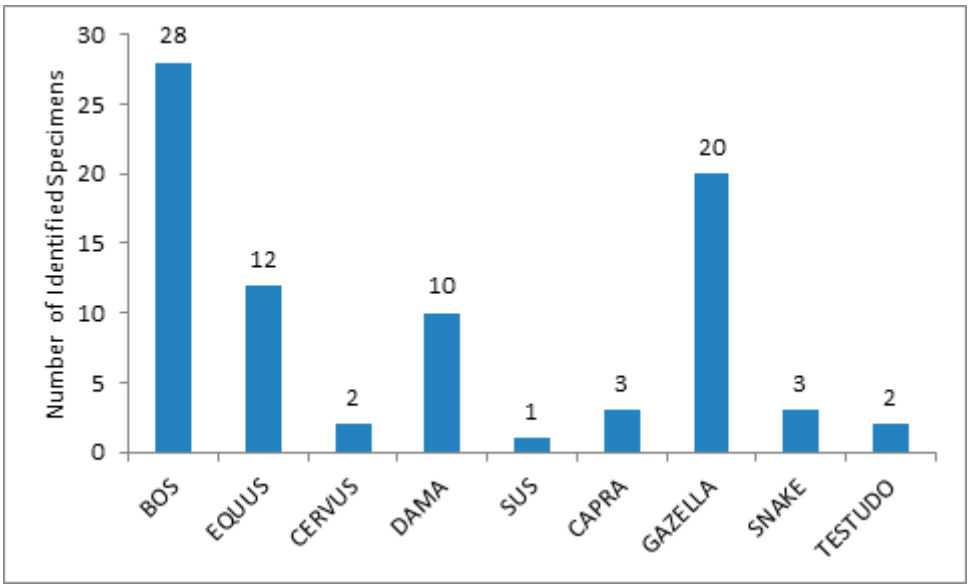

Table 1. Taxonomic composition in the Tinshemet Cave faunal assemblage.

EXCAVATION REPORT
MANOT CAVE

The 2018 Excavation Season at Manot Cave

Permit number G-51/2018

In collaboration with Ofer Marder[1] and Omry Barzilai[2]

[1] Department of Bible, Archaeology and Ancient Near East, Ben-Gurion University of the Negev, POB 653, Beer Sheva 84105, Israel

[2] Archaeological Research Department, Israel Antiquities Authority, P.O. Box 586, Jerusalem 91004, Israel

INTRODUCTION

Manot is an active karstic cave located in western Galilee, Israel. Its original entrance, situated at its westernmost part, seems to have collapsed circa 30,000 years ago, sealing the archaeological layers within. Previous seasons (2010–2017) exposed a series of UP occupations, while also indicating the presence of a Middle Paleolithic (MP) industry scattered within the cave (Barzilai et al. 2012, 2014, 2016; Herskovitz et al. 2015, 2017; Marder et al. 2013, 2017).

The paleoclimate conditions in the Manot Cave surroundings from 51-27 ka BP were studied based on the oxygen ($\delta^{18}O$) and carbon ($\delta^{13}C$) record of several stalagmites. $\delta^{13}C$ values of the speleothems suggest that the vegetation above the cave was mostly of C3 type with the development of very dense vegetation 36-27 ka BP (Yas'ur 2013). Superimposed on the general trend, short time-intervals were identified, in which harsh conditions developed. The sharp fluctuations in both $\delta^{18}O$ and $\delta^{13}C$ mainly between 35-27 ka BP points to frequent yearly and seasonal changes associated with period of global cooling.

Mountain gazelle (*Gazella gazella*) and Mesopotamian fallow deer (*Dama mesopotamica*) were most abundantly consumed at the site, respectively reflecting open landscapes and wooded environments (Schneller-Pels 2016; Orbach 2017). The micro-faunal record indicates mainly open landscapes, with a dominant presence of Guenther's Voles (*Microtus guentheri*; ca. 80% of the assemblage), alongside wood species such as *Apodemus spp*. (ca. 10%). Of interest are the remains of the Eurasian Snow Vole (*Chionomys nivalis*), which is limited today to Alpine environments (e.g., Mt. Hermon). Its existence supports the isotopic evidence suggesting occasional colder intervals during the EUP (Comay 2017), as does the isotopic analysis of *Patella* shells found within the cave (Bar-Yosef Mayer paper accepted). The botanical remains are dominated mainly by almond (*Prunus* cf. *amygdalus*). Deciduous oak (*Quercus ithaburensis*) remains were also found, which might reflect an open-park landscape (Marder et al. 2017).

Twelve excavation areas have been opened so far (A–L; Fig. 1), of which Areas C, E and I contain the best-preserved cultural layers. These areas display thick (about 2.5 m) stratigraphic profiles and extremely rich assemblages (Barzilai et al. 2012, 2014; Marder et al. 2013). While Areas E and I represent *in situ* occupations, the assemblages from Area C are found in secondary depositional contexts. Nevertheless, the chrono-cultural units in Area C are in agreement with the assumed stratigraphic order (Barzilai et al. 2016; Marder et al. 2017; Alex 2017).

This season, we aimed to refine our understanding on the Levantine Aurignacian sequence in the cave, and to allow re-sampling of some of the features, both for radiocarbon dating and for micro-morphological analysis. The excavations were confined to the areas closest to the original entrance to the cave, where the best preservation of archaeological remains was detected (Areas E and I), displaying *in situ* occupation layers.

In Area E, a focus was put on the excavation of Layers VI and IX, which proved to be very rich, displaying a thick accumulation of 30-40 cm each. In addition, an excavation was conducted in Area E2, with the purpose of establishing a stratigraphic affiliation to the hearth segment that was exposed there during the 2016 season.

In Area I, after reaching bedrock/extensive flowstone at the easternmost square, the excavations aimed to enlarge the collected assemblages in order to allow an established cultural affiliation.

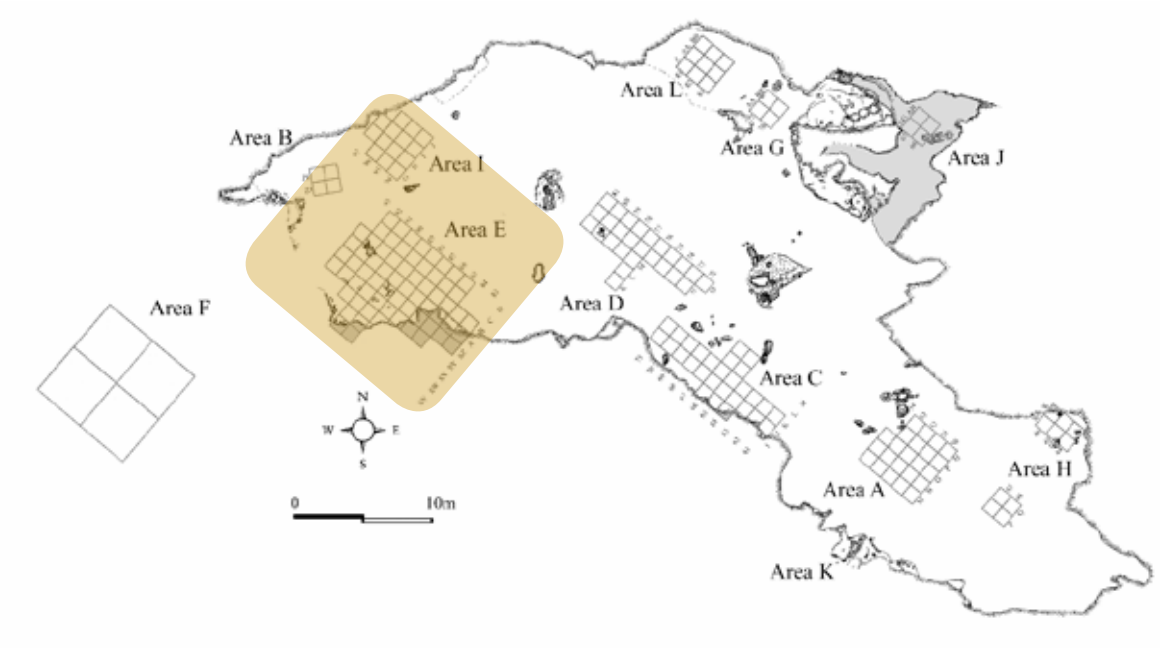

Figure 1: A general plan of the cave and the excavated areas. The areas excavated during the 2018 season are colored blue.

Area E

Area E is located at the southwestern part of the cave, at the top of the western talus. It is the closest to the estimated location of the original entrance to the cave, and is considered to represent a part of the main activity area. During the 2010-2017 seasons, nine distinct occupation layers were identified in Area E, defined, based on material culture remains, as Levantine Aurignacian (*senso lato*). During the 2018 season, the excavations in Area E were focused on four places (Fig. 2):

1. **The Middle Excavation Step (Squares SY-C 88-89)** – In order to further investigate Layer VI, which was partially exposed and sampled during the 2016 season. Preliminary analysis of the finds indicated that this is a rich layer, containing "classic" Levantine Aurignacian material culture. In order to refine our understanding of this occupation layer, the excavations aimed to expose the living surface that corresponds to a combustion feature L510, a multi-layered hearth uncovered in 2016. Additional objectives were the enlargement of our collections of material culture originating from "classic" Levantine Aurignacian contexts, to allow comparison to other sites in the region, and to collect additional samples for radiocarbon dating of this layer.

2. **The Lower (Southeastern) Excavation Step (Squares SY-A 86-87)**– in order to finish the removal of Hearth 522 and the find cluster associated with it, which were defined as Layer IX. The purpose of this excavation was to further investigate the find cluster exposed in square A87d during the 2017 season, suggested to be an older occupation layer – possibly Layer II-X.

3. **Area E2 (SV-SX 89-90)**. Area E2 was excavated during the 2016 season, following the southern and western contour of the cave's wall, trying to identify the location of the original entrance from within the cave. A large amount of Unit 1 soils were removed. Nevertheless, in square SW90 a possible hearth (L1701) was exposed towards the end of the season, but was not excavated. This season, the excavation in Area E2 was aimed to further investigate L1701, enlarge the finds assemblages associated with it, and refine our understanding of its stratigraphic position within the Area E sequence.

4. **Area E3 (A-B 83-84).** Area E3 was excavated during the 2017 season, with the purpose of following the southeastern cave wall, hoping to uncover additional human remains. At the end of the season, a cluster of finds, defined as Levantine Aurignacian, was partially revealed in Squares A-B 84. This season, excavations in Area E3 aimed to further expose the cluster of finds, trying to determine whether this is a small occurrence, possibly washed down from Area E, or an *in situ* layer of finds.

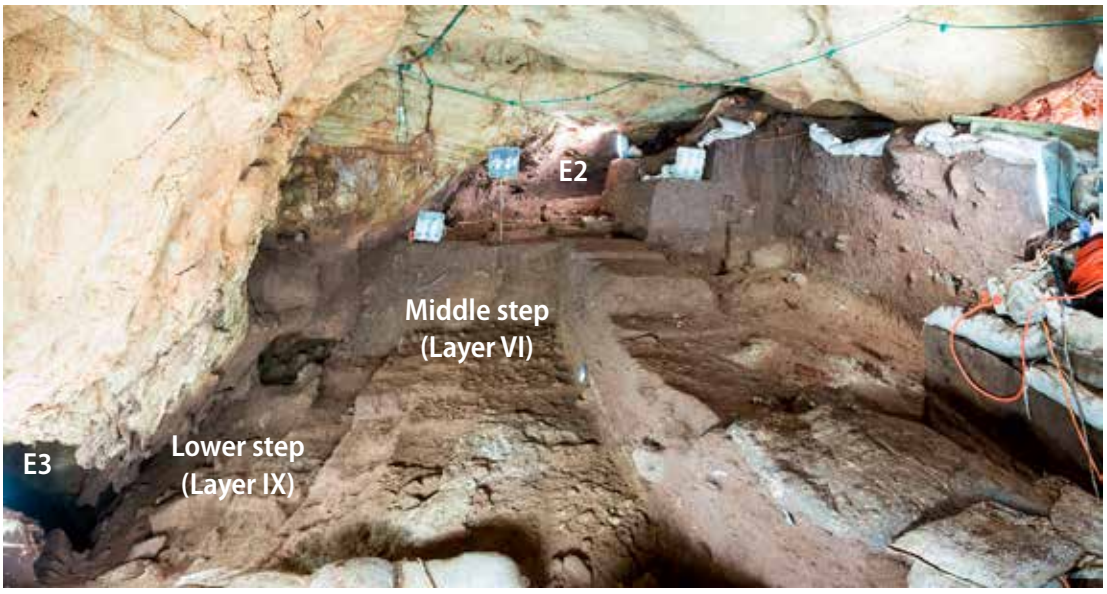

Figure 2: General view of Area E and the location of the 2018 excavations. Looking to the west.

Stratigraphy

No major changes were made to the stratigraphy as was defined in previous seasons. Nevertheless, following this season's excavation, both Layer VI and Layer IX were divided into sub-phases, counting three sub-phases each. The division was made based on the presence of soft sediment, containing low density of finds, between a series of find clusters associated with a single combustion feature. In Layer VI – a series of three clusters were associated with Hearth 510, in which at least three burning phases were identified. In Layer IX, three phases were identified in association to Hearth 522: 1) A dense accumulation of animal bones, overlaying and sealing L522 and probably representing a post-occupation activity (or probably a waste disposal of a later occupation layer). 2) Hearth 522 and associated find clusters. 3) Combustion feature L533, directly underlying Hearth 522, and associated find cluster. Accordingly, the find cluster identified during the 2017 season in Square A87c, which was suggested to be a part of a possible Layer II-X, was defined this season, as a part of Phase 3 (the oldest phase) of Layer IX. The revision was made due to the proximity of the two combustion features 522/533. Notably, this phase could represent an earlier occupation layer, but an analysis of the finds is required in order to establish such a distinction.

Layer VI (SY-C 88-89)

The excavation of Layer VI was conducted with the initial intention of allowing a wider exposure and further investigation of Layers VII and VIII, defined in previous seasons. However, Layer VI proved to be extraordinarily rich, and its excavation was therefore more time consuming than expected. Based on samples taken from the main combustion feature (L510), indicating at least three distinct burning phases, the excavation of Layer VI was conducted with an attempt to distinguish between possible corresponding occupation phases. The excavation focused on west of L510 (Squares SY-SZ 88-89; A 88). When identified, each find

cluster/occupation phase was exposed to as much area as possible and photographed before removed. Three such clusters were identified (L534, L535, L537), embedded in lightly cemented sediments, each occupying all of the excavated area. Between the clusters thin horizons (5-10 cm) of soft, yellowish-brown sediment were excavated, containing low densities of finds. These were regarded as natural sediment accumulations between occupation phases. At the end of the season, the exposure of the lower cluster (L537) was completed (Fig. 3), in preparation for its removal next season.

Figure 3: Hearth 510 (left) and associated occupation level. Looking to the southeast.

Coprolite Cluster L536 (B89a, b)

In the northeastern part of square B89, a cluster of hyenas' coprolites was uncovered, overlaying the earliest visible burning phase of Hearth 510 (Fig. 4). The cluster was exposed in a radius of 60 cm, and is probably extending into Square B90 to the northwest. The coprolites were found whole and in natural articulation, implying minimal post-depositional movements. Initial thoughts identified L536 as the continuation of L508, found and excavated in previous seasons and considered to represent hyena activity between occupation layers V and VI. However, unlike in L536, coprolites remains in L508, were found crushed and burned. Thus, both features do not bear any visible similarities.

L536 is therefore considered to represent a different activity rather than the one represented by L508. Its position overlaying the earliest visible burning phase of L510, raises questions regarding its stratigraphic correlation, "Was it a pit dug through the late burning phases of L510 or does L536 represent a short-term hyena activity between occupation phases in Layer VI? In order to try to answer these questions, excavations were conducted in Square C89. These are expected to proceed in the following season.

Figure 4: Coprolite cluster L536, Looking to the northwest.

Layer IX (SZ-A87)

In order to allow wider exposure of an underlying find cluster, exposed during the 2017 season, and defined as a possible Layer X, the excavation of Layer IX aimed to finish the removal of Hearth 522. The removal of Hearth 522 exposed an underlying combustion feature – L533. This is a small (~20 cm in diameter), very homogenous in concentration, which seems to have been dug into the underlying sediments. A small cluster of finds were exposed surrounding L533, also incorporating the cluster exposed during the 2017 season (Fig. 5). Although a thin layer of sediment separated the L522 and the 533 clusters, the exposure of both combustion features in the exact same location imply some continuity. Therefore, they are regarded as two phases of a single occupation layer (Layer IX). Nevertheless, radiocarbon ages and a more comprehensive analysis of the finds from each cluster are required in order to establish their cultural correlation.

Area E2

The excavation in Area E2 revealed a contact plain between the archaeological sediments (Unit 2) and the overlying Unit 1 sediments. It is sloping to the south and to the east, and is marked by the presence of large quantities small to medium size stones (Fig. 5, 6), alongside crusts with a small amount of charcoal fragments. The contact is sometimes hard to discern since the soil on both sides of the contact plain – below and above it – is basically the same colluvium of red soil coming from the outside of the cave. Live tree-roots penetrate through the soil of both units.

Figure 5: The contact plain between Unit 1 and Unit 2 sediments, in square SX90. Looking west.

The soil of the contact plain and underneath it was mostly soft, with some crusts, and a small amount of small stones. The soil contained many flint artifacts (mostly found during the wet sieving), bone fragments and coprolites (Fig. 6).

The most prominent feature in the area is the hearth L1701, which was identified in the previous season. The hearth lies on the contact plain between Unit 1 and Unit 2 and is part of this plain (Fig. 7).

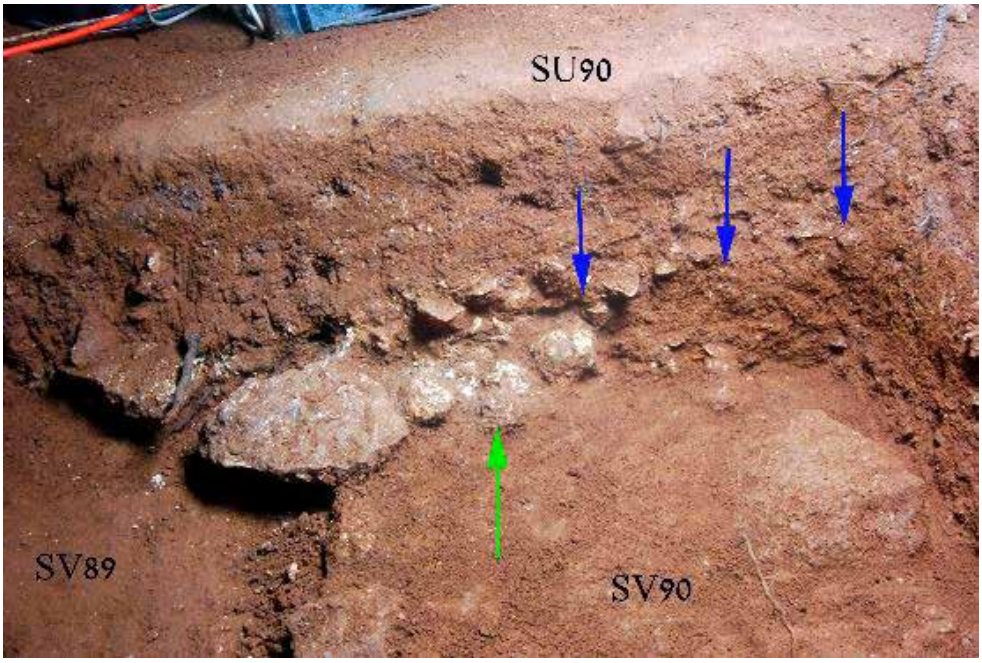

Figure 6: A concentration of coporlites (green arrow). The blue arrows indicate the sloping contact plain between Unit 1 on top and Unit 2 below, as seen in the section SV90/SU90, looking west.

Figure 7: Hearth L1701 with stones around it on the contact plain between Unit 1 sediments on top and Unit 2 archaeological sediments below. Looking west at squares SW90, SV90.

The hearth is about 0.7 m in diameter, built of gray powdery substance. The outer perimeter and top of this gray material is hardened and creates a very hard crust that covered and protected the soft gray sediments inside it. The gray sediments, probably wood ash, lies on top of red clay soil. The center of the hearth is about 11 cm high, thinning out to the rims of the crust (Figs. 8, 9).

Figure 8: L1701. The crusty rim of the hearth is visible. Looking west.

Figure 9: A section through L1701. Notice the red clay under the hearth. Looking west.

No dateable materials were found inside the hearth, but a charcoal sample – B17173 – was collected from the soil immediately underneath the hearth, sealed by the hard crust of the hearth. This sample should give a minimum age for the hearth.

Hearth L1701 and the contact plain corresponding to it were treated as a part of Layer I, defined in the main section of Area E. The association was made based on visual resemblance and on preliminary observation, which suggested some similarities between flint assemblages collected this, and in previous seasons. Nevertheless, no actual connection between the two was identified during the excavation. An examination of the finds is required to establish the stratigraphic position of L1701 within the Area E sequence.

Area E3 (Squares A-B 84-83)

Excavations in Area E3 aimed to better define the cluster of finds, exposed in the northern-most part of Squares A-B 84. For that purpose, the excavation was focused in the southern part of A-B 84, as well as in Squares A-B 83, trying to expose this find cluster on a larger area. This was done in order to see if the cluster exposed during the 2017 season is a local occurrence, or a part of a wider archaeological horizon.

A rich archaeological horizon was exposed in all of the excavated area in E3. Although the nature of deposition in these squares is still not clear (i.e. if this is an *in situ* accumulation or the result of post depositional processes – sediments drifted from one of the upper layers), the excavation yielded a rich flint and faunal assemblage, as well as a few charcoal samples for dating. Preliminary observations, based on the flint assemblage, are indicating a strong possibility that the finds in Area E3 represent a Levantine Aurignacian industry. Due to the topographic position of Area E3, separated from the main part of Area E by a stalactite and a thick flowstone cover, which create a natural "barrier" at the top of the steep slope of the western talus, these observations pose stratigraphic questions. Further work is required in order to determine whether the archaeological horizon exposed in E3 represents a lower, southern, habitation step or if it is the result of post depositional processes.

Area I

Area I is located along the cave's northern wall at the top of the western talus. During the last two seasons, a large combustion feature – L900 – was exposed in squares F94-F95. The aim this year was to continue the excavation of this feature in order to find out how deep it is, map and sample all its components, and to understand the extent and thickness of the hearth and associated archaeological layers.

At the end of the 2017 season, hearth L900 was removed, and a hard crust was exposed underneath it, covering most of square F94 and extending into square F95. The crust, named L900a, is of white/red color, highly cemented, and somewhat dome-shaped. The crust's thickness reached about 4 cm in the middle, thinning out at the edges. During the 2017 season a section of the crust was cut at the line between squares F94/F95 and revealed a distinct layer of flint implements lying under the crust.

The work concentrated mainly in Square F-94, with a small probe dug in F-95. The work was very slow and careful, most finds were recorded with a Total Station before removal, and a large block was removed for micro-morphological study.

The results of this season include the discovery of a deeper layer of the hearth, with an exceptionally good preservation of organic material, including the remains of burnt seeds. There was also a large cluster of flint artifacts, probably the largest concentration found in the living surfaces of Area I.

During the current season, the cemented crust of L900a was removed. Parts of it were very hard and required a hammer and a chisel to break through. Under the crust a layer of sandy-black, possibly burnt sediment was revealed (L900b; Fig. 10). It is about 4 cm thick, maybe thinning from the center outwards.

Figure 10: The full extent of L900b. Looking west.

L900b contains many flint artifacts, alongside burnt bones, many charcoal fragments, burnt seeds (Fig. 11) and a basalt piece. Many of the flint artifacts were mapped with a Total-Station measuring, as were most of the bone pieces and charcoals. There was a very high density of flint artifacts in layer L900b, much more than was found previously in the area.

Figure 11: A close-up look at the soil with the seeds. The white hard crust L900a is visible on the left.

During the excavation, most of layer L900b was removed. In sub-square F94b a very hard red sediment was exposed, which might be still a part of L900a. A layer of reddish clay underlie L900b. It was not excavated this season.

It seems that L900b represents an earlier phase of hearth L900. The very hard and thick crust that formed on top of L900b preserved very uniquely, a rich assemblage of finds. The number and density of the flint artifacts is remarkable. The recording of many pieces with a Total-Station will allow the presentation of the density and distribution of these finds.

The hearth was a little more than 1 meter in diameter, covering most of square F94 and the southern part of square F95. Some of the material excavated in F95c and F95d in 2017 probably belong to L900b as well. It seems that the hearth was levelled with the top of a big rock situated in square G94, which may be part of the bedrock.

REFERENCES

Barzilai, O., Avner, A., Bar-Mathews, M., Bar-Oz, G., Boaretto, E., Berna, F., Frumkin, A., Hershkovitz, I., Khalaily, H., Marder, O., Weiner S. and Yeshurun, R. 2012. Manot Cave: A Prehistoric Cave site in the Western Galilee. *Hadashot Arkeologiot* 124. http://www.hadashot-esi.org.il/report_detail_eng.asp?id=2183.

Barzilai, O., Marder, O. and Hershkovitz, I. 2014. Manot Cave, seasons 2011–2012. *Hadashot Arkeologiot* 126. http://www.hadashot-esi.org.il/Report_Detail_Eng.aspx?id=6470&mag_id=121.

Barzilai, O., Hershkovitz, I. and Marder, O. 2016. The Early Upper Paleolithic Period at Manot Cave, Western Galilee, Israel. *Journal of Human Evolution* 31 (1-2): 85-100.

Hershkovitz, I., Marder, O., Ayalon, A., Bar-Matthews, M., Yas'ur, G., Boaretto , E., Caracuta, V., Alex, B., Frumkin, A., Goder-Goldberger, M., Gunz, P., Holloway, R., Latimer, B., Lavi, R., Matthews, A., Slon, V., Bar-Yosef Mayer, D., Berna, F., Bar-Oz, G., Yeshurun, R., May, H., Hans, M., Weber, G. and Barzilai, O.

2015. Levantine cranium from Manot Cave (Israel) foreshadows the first European modern humans. *Nature* 520: 216-219.

Herskovitz, I., Latimer, B., Barzilai, O. and Marder, O. 2017. Manot 1 calvaria and recent modern human evolution: an anthropological perspective. *Journal Bulletins et Mémoires de la Société d'Anthropologie de Paris* 29: 119-130.

Marder, O. Alex, B., Avner., A. Bar-Mathews, M. Bar-Oz, G., Bar-Yosef-Mayer, D., Berna, F., Boaretto, E., Caracuta, V., Frumkin ,A., Goder-Goldberger, M., Hershkovitz, I., Latimer, B., Ron, l., Weiner, S., Weiss, U., Yeshurun, R. and Barzilai, O. 2013. The Upper Palaeolithic of Manot Cave, Western Galilee, Israel: the 2011-12 excavations. *Antiquity,* 87 (337), September 2013. http://antiquity.ac.uk/projgall/marder337.

Marder, O., Hershkovitz, I. and Barzilai, O. 2017. The Early Upper Palaeolithic period at the Manot Cave, Western Galilee: chrono-cultural, subsistence and palaeoenvironmental reconstruction. In: Y. Enzel and O. Bar-Yosef (eds.), *Quaternary Environments, Climate Change and Humans in the Levant*. Cambridge University Press, Cambridge. Pp. 267-276.